

INFLUENCE OF THE COMBINED VACUUM HEAT TREATMENT AND ELECTRON BEAM SURFACE MODIFICATION ON THE ELASTIC-PLASTIC BEHAVIOR OF Ti5Al4V ALLOY

YANKOV Emil¹, NIKOLOVA Maria P.¹, PETROV Petar², ZAHARIEVA Vanya¹, VALKOV Stefan²,
ORMANOVA Maria²

¹University of Ruse "A. Kanchev", Department of Material Science
and Technology, Bulgaria, EU

eyankov@uni-ruse.bg

²Bulgarian Academy of Sciences, Institute of Electronics,
Sofia, Bulgaria, EU

Abstract:

The improvement of the tribological behavior of the titanium alloys used for hard implants requires the application of different treatments (heat treatment and electron beam surface modification (EBSM) by scanning electron beam) that homogenize the bulk and surface structure as compared with the as-received material. In view of analyzing the influence of the applied vacuum heat treatment on Vickers hardness in three mutually perpendicular planes of the Ti5Al4V samples in as-received, quenched and quenched and precipitated condition are used for determining the plane for scratch test analysis and application of the EBSM afterward. The aim of this study is to reveal the changes in the mechanical properties (hardness, the coefficient of friction (μ) and tangential force (F_t) at a progressive loading of the normal force (F_N) up to pre-defined maximal value. The scratch results compare the heat treated and EBSM samples in different conditions in the rolling directions of testing. Such studies will be useful for further examinations of the alloy.

Keywords: Hardness, scratch, resistance to plastic deformation, concentrated energy fluxes

1. INTRODUCTION

The deposition of appropriate coatings or surface modifications together with a proper treatment of the substrate material are the decisive factors of the long-term stability of a hard implant for the orthodontic and dental application. If the alloy material is soft the surface film tends to fragmentize or dip into the implant that leads to fast wear of the surface, low internal fixation, and early implant failure. The wear of the surface due to the mechanical loading triggers electrochemical processes because of the different conductivity of the surface-substrate materials. That fact together with a poor osseointegration that accelerates corrosion [1], could cause inflammatory reactions to occur. One way of raising the long-term stability of the implant is to enhance the hardness of the material through heat treatment or/and additional modification of the surface with the help of concentrated energy fluxes like laser [2-4], electron beam [5, 6] etc. In the particular study, the possibility for enhancement of the mechanical properties of Ti5Al4V alloy through a combination of vacuum heat treatment and electron beam surface modification (EBSM) is studied. The examinations used for evaluating the elastic-plastic behavior of the alloy are hardness measurements and scratch tests for determining the change in the coefficient of friction (μ), tangential force (F_t) and resistance to plastic deformation (RPD).

2. MATERIALS AND EXPERIMENTAL PROCEDURES

Samples with dimensions 14×14×4 mm were cut out of 16 mm thick sheet material using the electroerosion cutting method. The chemical composition of the alloy given in **Table 1** was measured by JEOL JXCA-733 Microprobe scanning electron microscope (SEM) coupled to a WDX detector. The focused electron beam with 50 μ m diameter was operated at 19.9 kV for the acquisition of the chemical composition.

The as-received alloy samples were single solution treated (ST) for 30 min at 920 °C and water quenched. Half of the specimens were precipitated (P) for 4 hours at 500 °C and air cooled. All treatments were carried out in ≤ 1 Pa vacuum. The surfaces of the samples were grounded and polished before the EBSM.

Table 1 Chemical composition (in wt.%) of the Ti5Al4V alloy

	Al	V	Fe	Mn	Co	Cr	Mo	Pd	Nb	Hf	Ti
Ti5Al4V	5.212	4.403	0.139	0.113	0.065	0.002	0.174	0.153	0.363	0.036	Bal.

To study the effect of the surface treatment the Electron beam surface modification (EBSM) was applied to as-received, solution treated (ST) and ST and precipitated (ST+P) samples. The EBSM was carried out by electron beam installation Leybold Heraus (EWS 300/15-60). The following technological parameters were applied: electron beam current $I = 20$ mA, accelerated voltage $U = 52$ kV, speed of the samples motion $v = 0.5$ cm/s, electron beam frequency $f = 1$ kHz, electron beam diameter $d = 0.5$ mm and linear manner of scanning.

A Vickers Hardness tester 432 SVD by Wilson-Wilpert was used for the hardness measurements [7] by a load of 10 kg, dwell time of 10 s and distance 500 μm between the indents. The cross-section hardness of the EBSM samples was measured by 300 g load up to 500 μm depth from the surface. The scratch tests were performed on the rolling direction (perpendicular to the strips) of the samples with a CSM REVETEST Scratch Macrotester equipped with a Rockwell C diamond indenter with 200 μm tip radius and digitalized by 16-FMME-02 project [8]. Progressive load scratching mode with normal force range of 0 N to 30N was used in the experiments at a speed of 10 N/mm. The scratch track was evaluated using optical methods as well as by means of digital-signal records of the friction coefficient (μ) and tangential force (F_t). The light optical microscopy of the scratch tracks was performed using a Nikon microscope after Kroll's reagent etching the samples. The 14-megapixel digital camera was adapted to the microscope and used for the image acquisition.

The resistance to plastic deformation (RPD) was evaluated by the equation $RPD = F_N/A$ [9], where F_N is the normal force at maximal loading (30 N) and A is the area under the indenter.

3. RESULTS AND DISCUSSIONS

The results of the hardness measurements (**Figure 1**) in three mutually perpendicular planes - rolling direction (RD), normal direction (ND) and the top surface of the as-received, ST and ST+P showed differences because of the residual plastic deformation after rolling. Despite the heat treatment made, full recrystallization does not occur. The highest hardness value of the ST sample was measured in the RD where the hardness increased by 15.9 % as opposed to the as-received RD plane (**Figure 1a**). In the other two planes, the hardness changed by 16 % and 18.5 % for the top surface and ND, respectively. This difference was caused by the higher amount of occurring structural changes in both planes. In the case of the ST+P, this trend had continued and the changes were equal to 20 %, 21 % and 24.5 % for the RD, plan, and ND, respectively. After the EBSM (**Figure 1b**) the surface hardness of the as-received sample increased by 15 %, which was higher than the strengthening of the ST sample where the hardness grew by 13.5 %. For the ST+P sample, the hardness change after the EBSM was insignificant. The penetration depth of the Vickers indenter varied within the range of 31 μm (for the ST and ST+P) and about 34 μm (for the as-received) when measuring the hardness of the EBSM samples in the RD.

The highest hardness of all three samples was measured in the RD which was selected for the tribological tests. The RD was used for determination of μ coefficient of the as-received, ST and ST+P samples (**Figure 2a**). It could be observed that for the as-received sample the μ showed low initial values because of the fibrous texture (**Figure 4a**) and low hardness value. With the increase in load from 5 N to 30 N the μ trend unevenly fluctuated and varied from 0.3 up to 0.48. This phenomenon could be explained by the crossing of the indenter of differently structured stripes. The lamellar morphology reflects the F_t trend (**Figure 2c**). The

latter followed a progressive growth. The F_t fluctuations weakened with the increase of load because of the higher penetration of the indenter in depth.

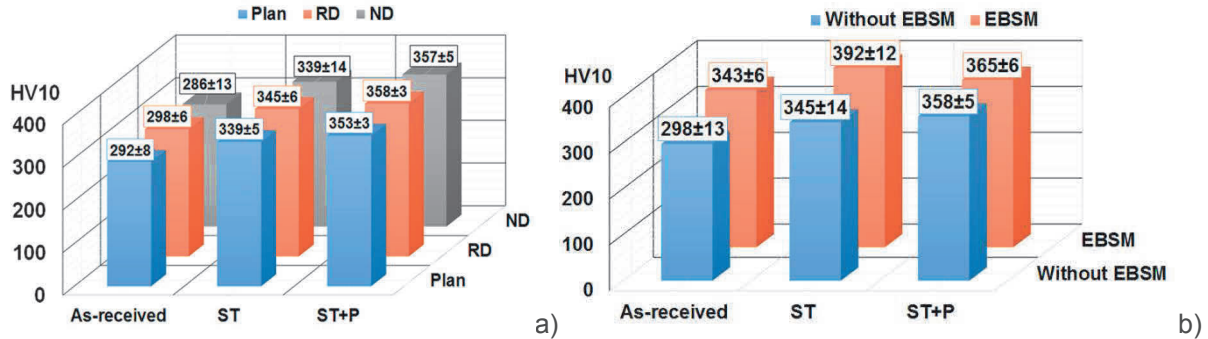


Figure 1 Average hardness values measured at a) three mutually perpendicular directions of the as-received, ST and ST+P samples; b) comparison of the average hardness values in the rolling direction of the specimens before and after the EBSM

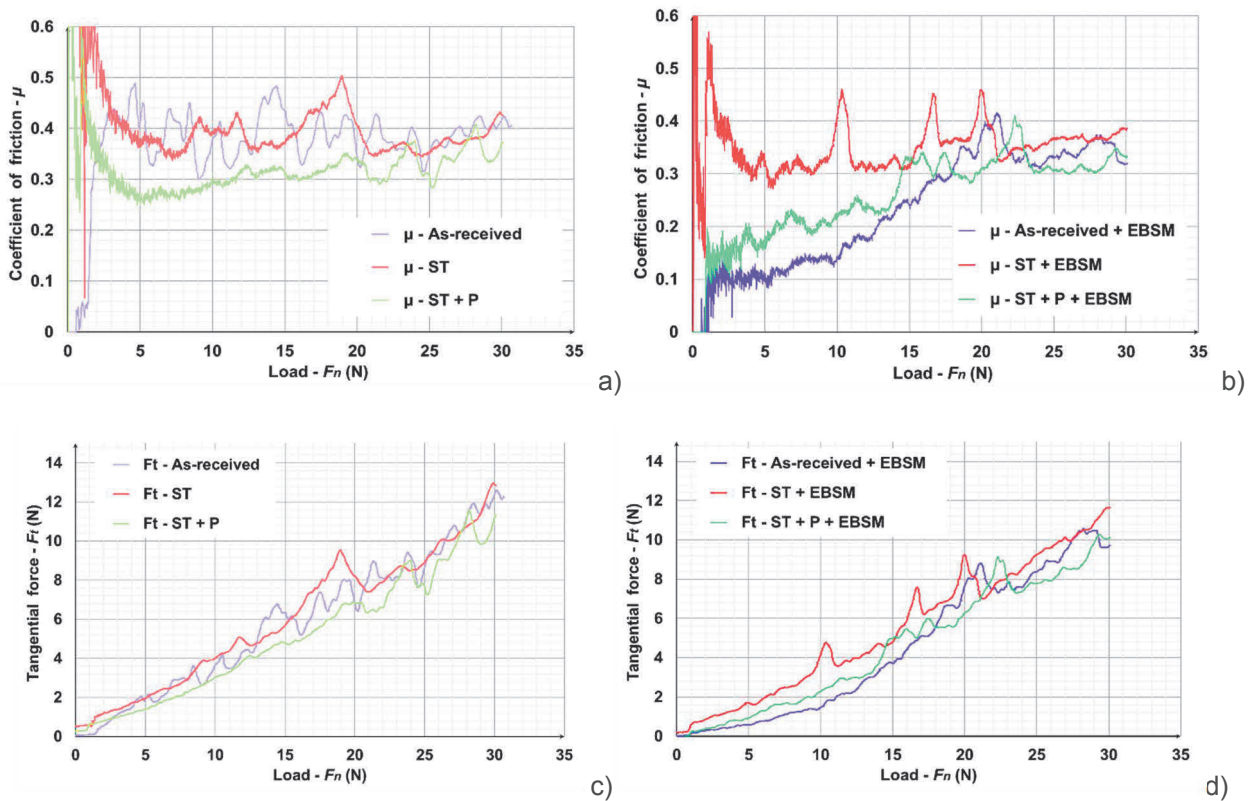


Figure 2 Comparison of the tangential force (F_t) and coefficient of friction (μ) during progressive 0 N to 30 N scratch test: a) μ of the as-received and heat treated samples; b) μ of the EBSM samples; c) F_t of the as-received and heat treated samples; d) F_t of the EBSM samples

The μ showed high initial values for the ST sample (**Figure 2a**) because of the higher surface hardness of the alloy and after 5 N the fluctuations were smaller. At about 19 N the μ increased and dropped sharply because of the local decrease in the sub-surface hardness (**Figure 3d**). The μ tendency was similar to those of the as-received sample and ranged about 0.4. After quenching F_t increased almost evenly (**Figure 2c**) due to the more homogenous and coarse structure but it indicated higher values in the entire interval up to 30 N. After

ST+P (**Figure 2a**) μ showed the lowest values and fluctuations because of the refined by the precipitates harder structure. Therefore, the precipitation will increase the durability of the alloy. F_t also showed the lowest values in almost whole examined loading range (**Figure 2c**) suggesting that the working resistance of the material in ST+P condition would be the lowest.

After the EBSM with this certain values of the parameters, the depth of the surface impact was about 263, 328 and 341 μm (determined at cross-sections micrographs) for the as-received, ST and ST+P, respectively, which influenced the in-depth hardness (**Figure 3d**) and μ values (**Figure 2b**). The lowest was the μ trend for the as-received+EBSM sample and it steadily increased up to 21 N. Similar in character μ trend was observed for the ST+P+EBSM sample where the starting values were also low. This effect in the μ trends of both specimens could be attributed to the surface grain refinement (**Figure 4 d, f**) and phase transformations occurring deeper in the substrates. The highest μ fluctuations and values were determined for the ST+EBSM specimen. The electron-beam treatment influenced its F_t values (**Figure 2d**) in a way similar to the changes in the μ trend.

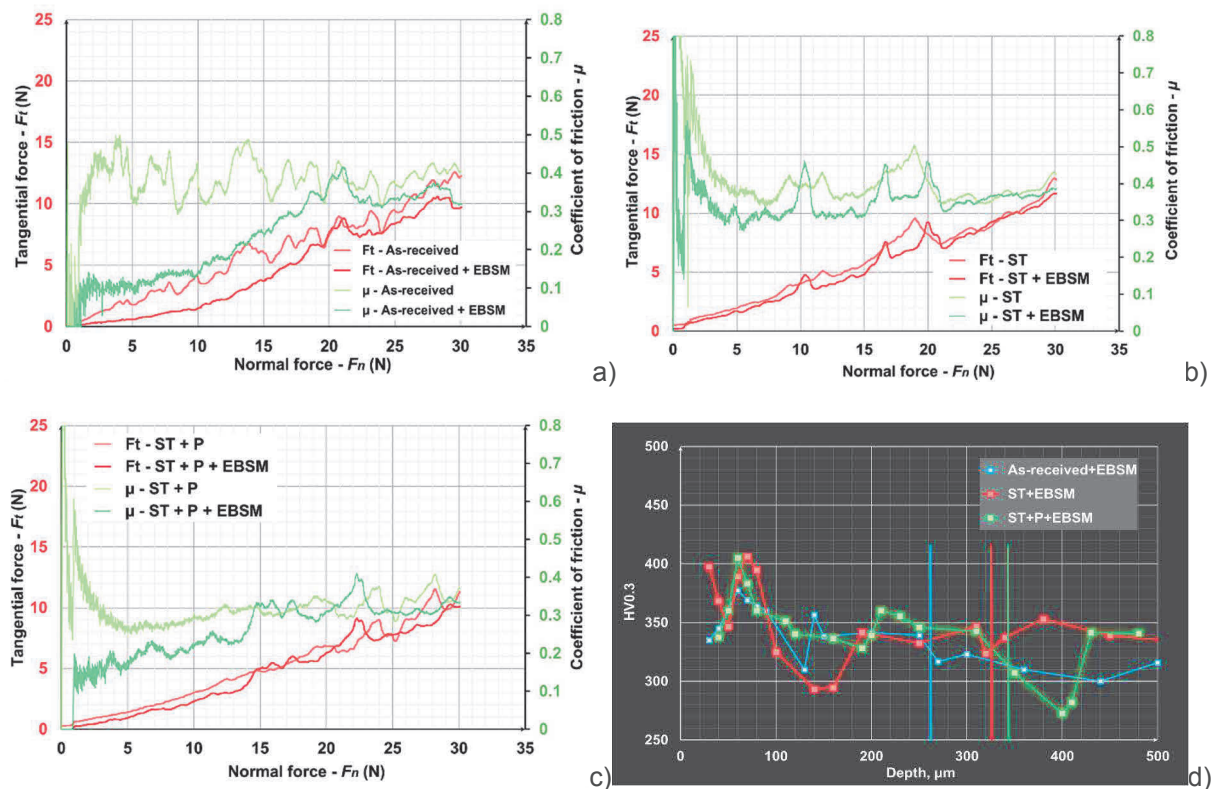


Figure 3 Comparison of the tangential force (F_t) and coefficient of friction (μ) during progressive 0 N to 30 N scratch test of: a) as-received and as-received+EBSM sample; b) ST and ST+EBSM sample; c) ST+P and ST+P+EBSM specimen; d) cross-section hardness of the as-received, ST and ST+P samples after EBSM

To get a comprehensive view of the changes occurring in the alloy after the different treatments, three comparative diagrams indicating $\mu = f(F_N)$ and $F_t = f(F_N)$ for all examined specimens are shown in **Figures 3a, b, and c**. For the as-received sample (**Figure 3a**) a clear decrease of μ in the range of 0 N up to 20 N was noticeable. This implies that the EBSM of the as-received material enhances its surface properties significantly. Under anormal load of 20 N - 30 N the treatment influence decreased because of the penetration of the indenter in the area of lower hardness (**Figure 3d**). The change in F_t trend up to 21 N was comparatively even that points a higher surface toughness compared to the untreated material. The μ and F_t trends followed the highest positive change of all EBSM samples. In the case of the ST alloy (**Figure 3b**), the changes after EBSM were the smallest. Regardless of this, μ and F_t tendencies of the EBSM sample displayed slightly lower values than

those of only ST specimen. This fact suggests that the EBSM treatment produces new surface structure but with similar morphology and mechanical properties. The μ upward trend continued until 20 N loading and after that the effect of the surface modification disappeared. In the initial phase up to 15 N load an essential improvement of the μ and F_t after the EBSM of the ST+P sample was seen (**Figure 3c**), where these parameters showed lower values. Despite the greater depth of the modified area, the EBSM after the precipitation had a little effect applied to the as-received and ST samples. This indicates that the obtained structure after ST+P+EBSM with the certain values of the parameters possesses lower durability than the other two electron-beam treated samples. At load value of between 20 N and 30 N the indenter penetrated deeper in the substrate and the surface treatment effect was lost.

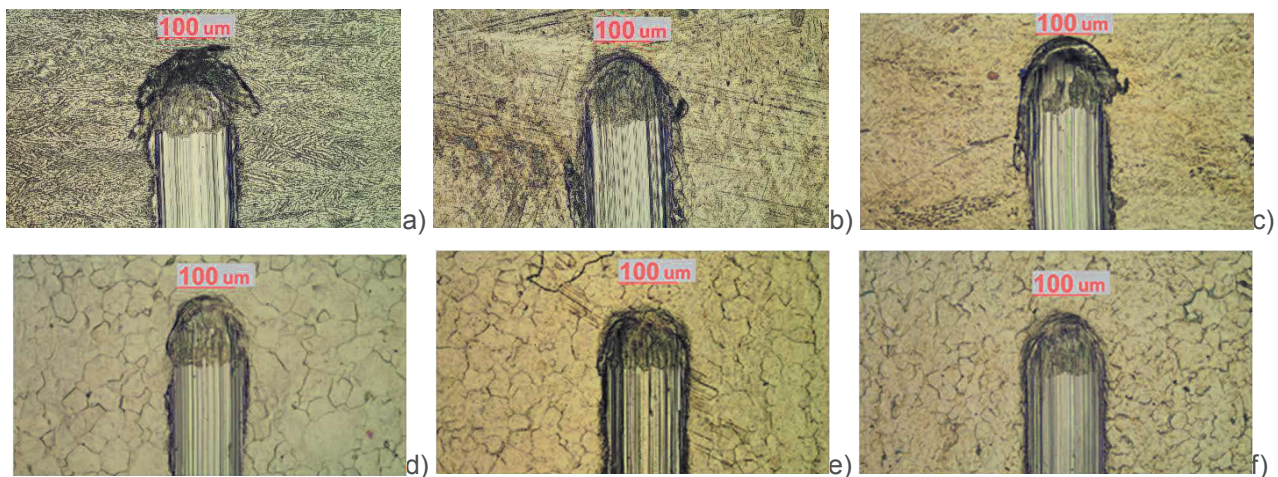


Figure 4 Micrographs of the scratch track ends of progressive 0 N - 30 N test of: a) as-received; b) ST; c) ST+P; d) as-received+EBSM; e) ST+EBSM; f) ST+P+EBSM samples

The changes in the μ and F_t values could be attributed to the microstructural characteristics of the as-received, heat treated and EBSM samples. The micrograph of the scratch track end of the as-received sample (**Figure 4a**) indicated cutting plastic deformation [10] after the indenter which explained the high RPD reaching a value of 52 MPa. This high measured value was due to the elastic component of the deformation that reduced the width of the scratch track end after unloading. After quenching the end of the scratch track showed wedge-forming plastic deformation [10] with low piling-up of material in front of the indenter. The RPD value of the ST sample (**Figure 4b**) was equal to 49 MPa at 30 N loading. For the ST+P alloy (**Figure 4c**) the straightening precipitates increased the RPD value up to 55 MPa at 30 N. For the as-received and heat treated samples the penetration depth of the indenter did not exceed 20 μm . The EBSM changes the surface structure that improves the mechanical properties of the alloy. For the as-received+EBSM sample, the RPD was rising to 60 MPa or it increased by 13 % as opposed to the as-received sample. The electron-beam treatment changed the way of plastic deformation from cutting into ploughing as seen in the scratch track micrograph (**Figure 4d**). For the ST+EBSM the RPD values increased by 1.5 % compared to the ST alloy which was confirmed by the similar micrograph of the track ends. In the case of the ST+P+EBSM, the RPD achieved a value of 57 MPa or it increased by 3.2 % as opposed to the ST+P sample. For the EBSM samples, the penetration depth of the indenter reached a value of 12.6 μm . The differences in the hardness values and the parameters defined by the scratch tests refer to the distinctions in the depth of examination and in-depth hardness values obtained after the EBSM.

4. CONCLUSION

The examined vacuum heat treatment processes enhance the surface hardness values by 16.77% and 21.84 % for the ST and ST+P, respectively and after EBSM these values additionally rises up by 13.49%

(overall 30%) and 2% (overall 23.8%) for the ST+EBSM and ST+P+EBSM, respectively. The most favorable effect of the EBSM with the certain values of the parameters on the tribological performance of the alloy is observed for the as-received sample. The surface treatment less affects the ST specimen. The EBSM changes the surface morphology which affects the μ trends, especially in the case of the as-received sample. These first successful outcomes for the enhanced mechanical properties of the implant alloy suggest the need for further research to establish the optimum parameters for EBSM in order to increase the surface toughness of the $\alpha+\beta$ titanium alloy. Additional metallographic, phase and tribological analysis are necessary to explain the surface changes as well as additional surface treatments for improvement of the surface properties of the alloy are needed to be explored.

ACKNOWLEDGEMENTS

The financial support of this work was provided by the National Science Fund of Ministry of Education and Science, Bulgaria, under Grant project "Gradient functional nanocoatings produced by vacuum technologies for biomedical applications" with number DN $\text{\textcircled{R}}$ 07/3 (2016).

REFERENCES

- [1] MANAM, N. S., HARUN, W. S. W., SHRI, D. N. A., GHANI, S. A. C., KURNIAWAN, T., ISMAIL, M. H., IBRAHIM, M. H. I. Study of corrosion in biocompatible metals for implants. *Journal of Alloys and Compounds*, 2017, vol. 701, pp. 698-715, <https://doi.org/10.1016/j.jallcom.2017.01.196>.
- [2] KATAHIRA, K., EZURA, A., OHKAWA, K., KOMOTORI, J., OHMORI, H. Generation of bio-compatible titanium alloy surfaces by laser-induced wet treatment. *CIRP Annals - Manufacturing Technology*, 2016, vol. 65, pp. 237-240, <https://doi.org/10.1016/j.cirp.2016.04.053>.
- [3] YAN, C., HAO, L., HUSSEIN A., WEI, Q., SHI, Y. Microstructural and surface modifications and hydroxyapatite coating of Ti-6Al-4V triply periodic minimal surface lattices fabricated by selective laser melting. *Mater Sci Eng C Mater Biol*, 2017, vol. 75, pp. 1515-1524, doi: 10.1016/j.msec.2017.03.066.
- [4] AKKAN, C. K., HÜRB, D., UZUN, L., GARIPCAN, B. Amino acid conjugated self assembling molecules for enhancing surface wettability of fiber laser treated titanium surfaces. *Applied Surface Science*, 2016, vol. 366, pp. 284-291, <https://doi.org/10.1016/j.apsusc.2016.01.083>.
- [5] SIDAMBE, A. T. Biocompatibility of Advanced Manufactured Titanium Implants - A Review. *Materials*, 2014, vol. 7, pp. 8168-8188, doi:10.3390/ma7128168.
- [6] OKADA, A., UNO, Y., UEMURA, K., RAHARJO, P., MCGEOUGH, J. A. Surface modification for orthopaedic titanium alloy by wide-area electron beam. *Journal of Engineering Manufacture. Proceedings of the Institution of Mechanical Engineers*, 2007, vol. 221, pp. 173-178, DOI: 10.1243/09544054JEM574.
- [7] YANKOV, E., NIKOLOVA, M. Changes in the mechanical properties and microstructure of anisotropic austenitic stainless sheet steel after uniaxial tensile test. In *Manufacturing Engineering - CoSME'16*. Brasov: Romania, 2017, vol. 94, ISSN 2261-236X; DOI: 10.1051/mateconf/20179402017.
- [8] YANKOV, E. et al. Project: Development and improvement of specialized equipment for microstructural and tribological analysis by digitalization of the received information. In Supported by Scientific Researches Fund of University of Ruse "A. Kanchev"; <http://nis.uni-ruse.bg/FMT-16/#MT-2>;
- [9] WETTER, R. *The interplay of System Dynamics and Dry Friction: Shakedown, Ratcheting and Micro-Walking*, Thesis, Berlin, 2016, 132 p., DOI: 10.14279/depositonce-5000;
- [10] HUTCHINGS, I. M. *Tribology - Friction and Wear of Engineering Materials*. University of Cambridge, UK, 1992, 280 p., ISBN: 9780340561843.